

PROCEEDINGS OF SPIE

SPIDigitalLibrary.org/conference-proceedings-of-spie

Parking sensor-inspired approach to photoacoustic-guided hysterectomy demonstrated with human cadavers

Wiacek, Alycen, Wang, Karen, Wu, Harold, Lediju Bell, Muyinatu

Alycen Wiacek, Karen C. Wang, Harold Wu, Muyinatu A. Lediju Bell, "Parking sensor-inspired approach to photoacoustic-guided hysterectomy demonstrated with human cadavers," Proc. SPIE 11642, Photons Plus Ultrasound: Imaging and Sensing 2021, 116420T (5 March 2021); doi: 10.1117/12.2579023

SPIE.

Event: SPIE BiOS, 2021, Online Only

Parking sensor-inspired approach to photoacoustic-guided hysterectomy demonstrated with human cadavers

Alycen Wiacek^{a,*}, Karen C. Wang^b, Harold Wu^b, and Muyinatu A. Lediju Bell^{a,c,d}

^aDepartment of Electrical and Computer Engineering, Johns Hopkins University, USA

^bDepartment of Gynecology and Obstetrics, Johns Hopkins Medicine, USA

^cDepartment of Biomedical Engineering, Johns Hopkins University, USA

^dDepartment of Computer Science, Johns Hopkins University, USA

ABSTRACT

Similar to the parking-assist sensors on modern automobiles, which alert drivers of impending impact to an object, we are developing an auditory photoacoustic-based guidance system to assist with avoidance of impending injuries to ureters during hysterectomy procedures. The contribution described in this paper considers international standards for medical alarms. The system was demonstrated during both open and laparoscopic hysterectomy procedures on two human cadavers. Using methylene blue to enhance ureter contrast, the proximity of a surgical tool tip to the ureter was measured using the visual information provided in photoacoustic images. Distance measurements were then successfully mapped to auditory signals, which increased in auditory frequency as the tool-to-ureter distance decreased to convey surgical tool proximity to the ureter. Fundamental frequencies increased from 150 Hz to 866 Hz for tool-to-ureter distances of 2.47 mm to 5 mm. These results are promising to assist with the avoidance of accidental ureteral injuries during hysterectomy and other procedures that suffer from similar challenges with regard to iatrogenic ureteral injuries.

1. INTRODUCTION

Surgical removal of the uterus requires the cauterization and transection of the uterine arteries while preserving the nearby ureters.¹ One challenge with this surgery is that the reported incidence rates of ureteral injury range 0.4%–1.7%^{2,3} for non-malignant conditions and can be as high as 4.7% for patients undergoing hysterectomy for malignant conditions.² These intraoperative injuries cause increased complications, including hospital readmission, sepsis, and death.² In addition, 67% of hysterectomies are performed laparoscopically, with or without robotic assistance,⁴ resulting in a 4.2 increase in the risk of ureteral injury with a minimally invasive hysterectomy when compared to an open approach.⁵

Previous work from our group demonstrated the feasibility a photoacoustic approach to hysterectomy in three stages. First, a custom photoacoustic light delivery system and robotic assistance was tested with a 3D printed blood vessel phantom.⁶ Second, the concept of injecting methylene blue into the ureter to distinguish the ureter from the uterine artery was validated in *ex vivo* experiments using plastic tubing filled with blood and methylene blue.⁷ Third, an open hysterectomy procedure was performed on a human cadaver and an auditory method was demonstrated to convey proximity information to surgeons.⁸ The work presented in this paper builds on our initial success with phantom experiments^{6,7} and open human cadaver experiments⁸ to demonstrate the proposed photoacoustic system laparoscopically. We additionally build on the previously proposed auditory feedback system⁸ by establishing an auditory alarm system while considering the International Electrotechnical Commission (IEC) standard for medical alarms (i.e., IEC 60601-1-8).^{9,10}

The auditory feedback system is inspired by a parking sensor in an automobile,^{11,12} where the distance between the vehicle and an object is tracked and an audible tone ensues as the driver approaches the object in order to alert the driver to the risk of impact, as depicted in Fig. 1. Similarly, we intend for the photoacoustic-based auditory feedback system to track the distance between the surgical tool and the ureter and beeping will ensue if the surgical tool approaches the ureter, in order to alert the surgeon of an impending risk of ureteral injury. This system has the potential to provide the real-time information needed to avoid accidental ureteral injuries during hysterectomies.

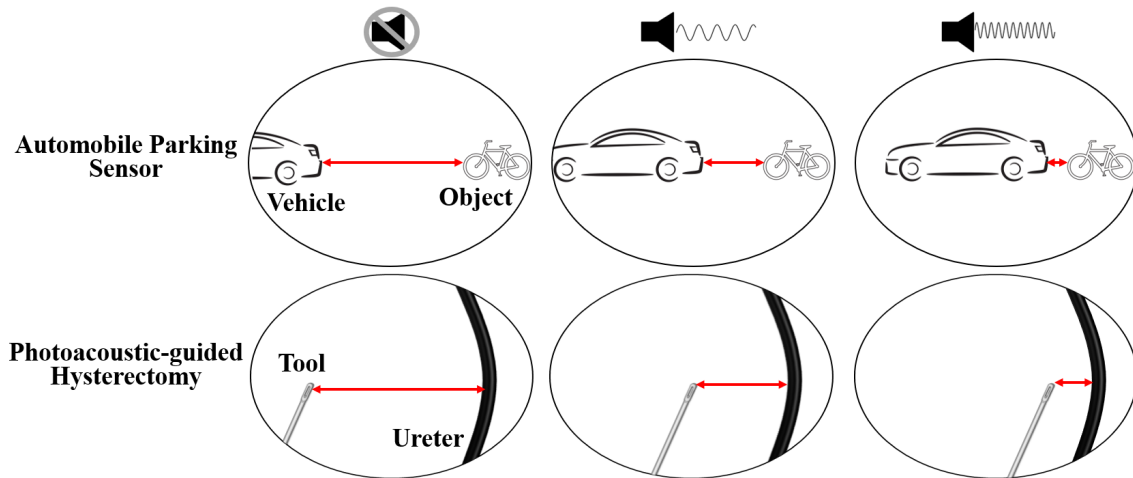


Figure 1. Diagram depicting the parking sensor-inspired approach to photoacoustic-guided hysterectomy where the vehicle and the tool are in motion and the object and ureter are stationary. The top row indicates the status of the auditory feedback, the second row shows our parking sensor inspiration, and the third row shows our surgical application. Initially (left) there is no sound, then as the target gets closer auditory feedback begins (center), which increases in frequency (right) as the distance decreases.

2. METHODS

2.1 Experimental Setup

A total of two human cadavers were utilized in this study for the open and laparoscopic procedures. During both procedures, the ureter and distal portion of the uterine artery were dissected and sutured at the distal end. The uterine artery was injected with whole human blood, and the ureter was filled with 400 μM and 200 μM methylene blue mixed with urine for the open and laparoscopic procedures, respectively. A Phocus Mobile laser (Opotek, Inc., Carlsbad, CA) operating at wavelengths from 690 nm to 800 nm with a pulse repetition frequency of 10 Hz was coupled to a 5 mm- or 2 mm-diameter fiber bundle emitting energies of 31.7 mJ or 16.6 mJ per pulse, respectively. During the open procedure, the fiber bundle was fixed with a ring stand. During the laparoscopic procedure the fiber bundle was attached to the surgical tool using a custom 3D printed adapter and inserted into a 12 mm trocar to avoid additional incisions. This setup was used to illuminate the ureter and uterine artery. Co-registered ultrasound and photoacoustic data were acquired using an Alpinion ECUBE12R research ultrasound scanner (Alpinion, Seoul, Korea), connected to an Alpinion EC3-10 transvaginal ultrasound probe, with a center frequency of 6 MHz.

2.2 Data Acquisition and Analysis

Ultrasound and photoacoustic channel data were acquired both with and without a laparoscopic grasper tool tip (Autosuture Endo Grasp, Medtronic, Fridley, MN) placed in the imaging plane. During the open procedure, with the laparoscopic tool in the imaging plane, the tool was navigated between the ureter and uterine artery. First, touching the ureter, then sweeping toward the uterine artery, and finally touching the uterine artery. This motion was then reversed and repeated for approximately 6 seconds. Co-registered ultrasound and photoacoustic videos of this motion were acquired with the goal of mapping proximity information to auditory cues.

Standard delay-and-sum (DAS) beamforming was used to create ultrasound images. Both DAS and short-lag spatial coherence (SLSC)^{13,14} beamforming were implemented to create photoacoustic images. Specifically, DAS beamforming was used to form dual-wavelength images, while SLSC beamforming was used when the tool was inserted into the imaging plane and to identify regions of interest (ROIs) during the laparoscopic investigation. Because SLSC beamforming directly displays the coherence of received signals, SLSC images offer improved visualization compared to DAS images when high-amplitude, incoherent artifacts are present. Each DAS or

SLSC photoacoustic image was normalized to its brightest pixel prior to display. Dual-wavelength images were formed by assigning blue and red colormaps to the photoacoustic images acquired with 690 nm and 750 nm wavelengths, respectively, then overlaying the color images on the grayscale ultrasound image.

2.3 Auditory Mapping

In order to convey proximity information to surgeons, we previously proposed an auditory mapping,⁸ enabling surgeons to focus on the surgical task, rather than divert their attention to additional monitors containing photoacoustic images. This mapping was initially performed without consideration of the IEC standard.⁹ Here we narrow the selected frequencies to the range specified, and we include the harmonics required by the IEC standard. In particular, the IEC standard⁹ specifies that the auditory alarm should have a fundamental frequency between 150 and 1,000 Hz, containing at least four harmonics in order to assist in localization of the signal and avoid other signals blocking it from perception. Therefore, this auditory cue starts at a fundamental frequency of $f_{\min} = 150$ Hz and increases in frequency up to $f_{\max} = 1000$ Hz when touching the ureter. In order to introduce the four required harmonics, the resulting signal was superimposed with frequencies (i.e., f_{harmonic}) at multiples of 2, 3, and 4 times the fundamental frequency, each with amplitude 10% of the signal at the fundamental frequency. The identified positions of the ureter and uterine artery were fixed while the surgical tool was tracked as the brightest pixel in each subsequent photoacoustic image.

Although two laser wavelengths are required to achieve the proposed system, the demonstration of feasibility of the auditory feedback system utilized a single wavelength, as the 10 Hz pulse repetition frequency of our laser system would reduce display rates to a level that would be limited to slower tool velocities. A system capable of faster tuning between 690 nm and 750 nm wavelengths would enable auditory feedback in real-time. However, to demonstrate tracking feasibility within our current system limitations, the position of tool tip, P_t , and the position of the ureter, P_u , were identified in photoacoustic images created with a single 750 nm laser wavelength, as the tool was navigated between the ureter and uterine artery (as described in Section 2.2). In particular, the position of the tool, P_t , was selected as the region surrounding the brightest pixel in the 750 nm image. The region identified as the surgical tool was assigned a green colormap, then temporarily removed from the image (i.e., set to zero). Next, with the tool region removed, the position of the uterine artery was selected as the region surrounding the brightest pixel in the remaining image. This region was assigned to a red colormap, then temporarily removed from the image (i.e., set to zero). Next, with both the surgical tool and uterine artery removed from the image, the position of the ureter, P_u , was defined as the brightest pixel in the remaining image. This region was then set to a blue colormap. The three colormaps (i.e., green, red, and blue) were then combined into a single image. Each identified region was normalized by its brightest pixel and displayed with a dynamic range that enhanced signal visualization.

The calculated Euclidean distance between the ureter and the tool (i.e., $\|P_u - P_t\|_2$) was temporally filtered to remove large changes in the derivative (i.e., velocity) that are not representative of the steady tool motion during this experiment. This distance was then used to create the auditory signal with the fundamental frequency defined as:

$$f_{\text{fundamental}} = \begin{cases} f_{\max} - \left(\frac{f_{\max} - f_{\min}}{t} \right) \|P_u - P_t\|_2, & \text{if } \|P_u - P_t\|_2 < t \\ 0, & \text{if } \|P_u - P_t\|_2 \geq t. \end{cases} \quad (1)$$

where t is a pre-defined distance threshold, and f_{\min} and f_{\max} are pre-defined frequency limits. If the operator was sufficiently far from the ureter (i.e., $t = 5$ mm in this study), no sound was played. As the operator approached the ureter, an auditory cue was initiated.

3. RESULTS

Figs. 2(a) and 2(b) show example dual-wavelength images from the open and laparoscopic procedures, respectively. In both images the ureter and the uterine artery are visualized and differentiated based on the presence of blue and red signals, respectively. Quantitatively, at 690 nm laser wavelength, the contrast difference between the ureter and uterine artery was 0.5 dB and 14.2 dB during the open hysterectomy and laparoscopic hysterectomy,

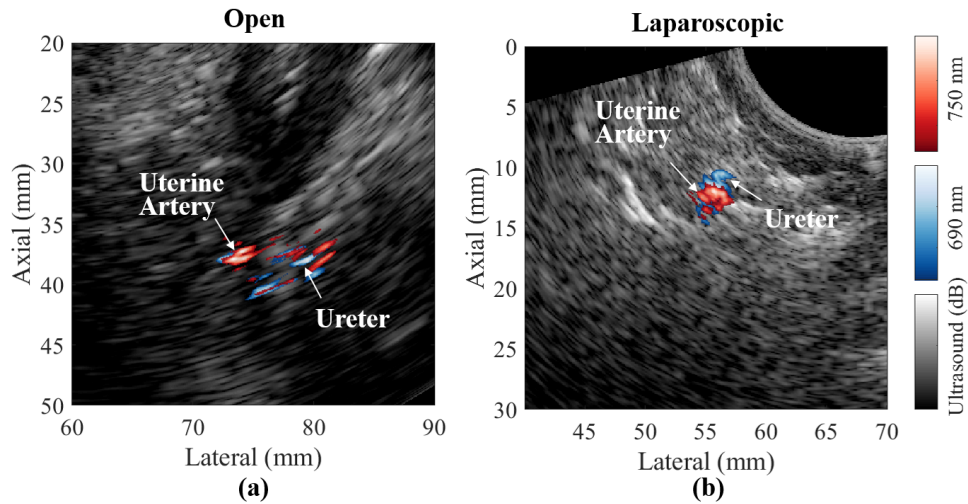


Figure 2. Dual-wavelength photoacoustic images acquired during the (a) open and (b) laparoscopic procedures within a human cadaver.

respectively. At 750 nm laser wavelength, the contrast difference between the ureter and uterine artery was 4.9 dB and 24.3 dB during the open hysterectomy and laparoscopic hysterectomy, respectively. For each procedure, the increase when comparing the contrast difference at 690 nm wavelength to that at 750 nm wavelength (i.e., the increase from 0.5 dB to 4.9 dB in the open procedure and from 14.2 dB to 24.3 dB in the laparoscopic procedure) is responsible for the differentiation of the ureter from the uterine artery in the dual-wavelength images. More specifically, this increased contrast difference enables the uterine artery to be visualized in the 750 nm image and differentiated from the ureter. Similarly, the ureter is visualized in the image acquired with 690 nm laser wavelength, because the contrast difference between the ureter and the uterine artery is smaller at 690 nm compared to that at 750 nm.

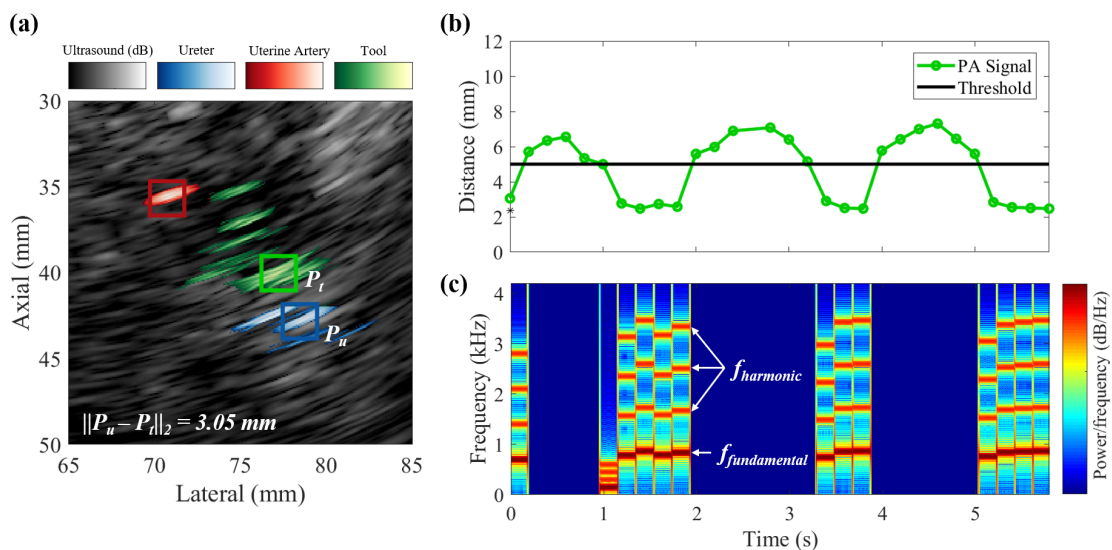


Figure 3. (a) Example photoacoustic image used to estimate the distance between the tool shown in green and the ureter shown in blue. (b) Calculated distance as a function of time. (c) Spectrogram derived from distance measurements, representing a visual display of the distance to auditory signal mapping.

Fig. 3(a) shows an example photoacoustic image with colored regions corresponding to the ureter, uterine artery, and tool shown in shades of blue, red, and green, respectively. Based on the assigned regions, the distance between the ureter and the tool for this example was 3.05 mm, as shown in the bottom left corner of the image. Artifacts surrounding the surgical tool are present in Fig. 3(a), however the automated tracking algorithm described in Section 2.3 is robust to these artifacts and tracks the brightest pixel only, which was identified as the tool tip.

Fig. 3(b) shows the photoacoustic-based distance calculation in green for the complete 6 s sequence of photoacoustic images. The solid black line indicates the $t = 5$ mm threshold for auditory feedback. The photoacoustic-based distances ranged from 2.47 mm to 7.31 mm.

Fig. 3(c) shows the spectrogram derived from the distance measurements in Fig. 3(b). The fundamental frequency is indicated by $f_{\text{fundamental}}$ and the harmonics of the fundamental frequency are indicated by f_{harmonic} . These fundamental frequencies range from 150 Hz to 866 Hz. The peaks in the spectrogram correspond to the valleys in the distance measurements and indicate a high frequency auditory cue alerting surgeons to the proximity of the tool to the ureter.

4. DISCUSSION AND CONCLUSION

The work presented in this paper improves previous demonstrations⁶⁻⁸ of a photoacoustic-based approach to guiding hysterectomies by introducing an auditory alarm system inspired by an automobile parking sensor, with consideration of the international standard for medical alarms.⁹ These results also highlight the importance of demonstrations in the realistic environment of a human cadaver prior to translation to patients.¹⁵ Dual-wavelength 690/750 nm images showed up to 4.9 dB and 24 dB contrast differences between the ureter and uterine artery during the open hysterectomy and laparoscopic hysterectomy, respectively.

Despite the absence of a fast-tuning system to achieve dual-wavelength imaging for the photoacoustic-based auditory cues, the results illustrated in Fig. 3 are promising for future development. These results nonetheless demonstrate the potential to bypass technological requirements for additional monitors containing photoacoustic images, which are ultimately based on the appearance of the metal surgical tool in the same photoacoustic image as another target (i.e., the ureter). This concept is not limited to hysterectomy procedures, and a similar auditory-based system has the potential to be implemented in other applications of photoacoustic-based surgical guidance that require proximity to critical structures, such as pedicle screw placement in spinal fusion surgeries,^{16,17} avoidance of the internal carotid arteries in endonasal transsphenoidal surgery,^{18,19} and targeting of major blood vessels for cauterization or avoidance of these blood vessels for tissue resection during abdominal surgery.²⁰ Future work will focus on the development of a fast-tuning system and investigate advanced spectral unmixing methods based on the acoustic frequency response²¹ to robustly identify regions of interest.

ACKNOWLEDGMENTS

This work was supported by a Johns Hopkins Discovery Award and NSF CAREER Award ECCS-1751522. The authors thank John Thate and Karl Storz Endoskope for the generous use of their laparoscopic equipment and Michelle Graham and Eduardo Gonzalez for their assistance during the cadaver studies. We additionally acknowledge support from the Johns Hopkins Carnegie Center for Surgical Innovation.

REFERENCES

- [1] Williams, P. L., Bannister, L., Berry, M., Collins, P., Dyson, M., Dussek, J., and Ferguson, M., "Gray's anatomy: the anatomical basis of medicine and surgery," *Edinburgh: Churchill Livingstone* **38**, 1560 (1995).
- [2] Blackwell, R. H., Kirshenbaum, E. J., Shah, A. S., Kuo, P. C., Gupta, G. N., and Turk, T. M., "Complications of recognized and unrecognized iatrogenic ureteral injury at time of hysterectomy: a population based analysis," *The Journal of Urology* **199**(6), 1540–1545 (2018).
- [3] Vakili, B., Chesson, R. R., Kyle, B. L., Shobeiri, S. A., Echols, K. T., Gist, R., Zheng, Y. T., and Nolan, T. E., "The incidence of urinary tract injury during hysterectomy: a prospective analysis based on universal cystoscopy," *American Journal of Obstetrics and Gynecology* **192**(5), 1599–1604 (2005).

- [4] Lim, P. C., Crane, J. T., English, E. J., Farnam, R. W., Garza, D. M., Winter, M. L., and Rozeboom, J. L., “Multicenter analysis comparing robotic, open, laparoscopic, and vaginal hysterectomies performed by high-volume surgeons for benign indications,” *International Journal of Gynecology & Obstetrics* **133**(3), 359–364 (2016).
- [5] Packiam, V. T., Cohen, A. J., Pariser, J. J., Nottingham, C. U., Faris, S. F., and Bales, G. T., “The impact of minimally invasive surgery on major iatrogenic ureteral injury and subsequent ureteral repair during hysterectomy: a national analysis of risk factors and outcomes,” *Urology* **98**, 183–188 (2016).
- [6] Allard, M., Shubert, J., and Bell, M. A. L., “Feasibility of photoacoustic-guided teleoperated hysterectomies,” *Journal of Medical Imaging* **5**(2), 021213 (2018).
- [7] Wiacek, A., Wang, K. C., and Bell, M. A. L., “Techniques to distinguish the ureter from the uterine artery in photoacoustic-guided hysterectomies,” in [*Photons Plus Ultrasound: Imaging and Sensing 2019*], **10878**, 108785K, International Society for Optics and Photonics (2019).
- [8] Wiacek, A., Wang, K. C., Wu, H., and Bell, M. A. L., “Dual-wavelength photoacoustic imaging for guidance of hysterectomy procedures,” in [*Advanced Biomedical and Clinical Diagnostic and Surgical Guidance Systems XVIII*], **11229**, 112291D, International Society for Optics and Photonics (2020).
- [9] International Electrotechnical Commission, “IEC 60601-1-8: Medical electrical equipment—General requirements, tests and guidance for alarm systems in medical electrical equipment and medical electrical systems,” (2006).
- [10] Edworthy, J., Reid, S., McDougall, S., Edworthy, J., Hall, S., Bennett, D., Khan, J., and Pye, E., “The recognizability and localizability of auditory alarms: Setting global medical device standards,” *Human Factors* **59**(7), 1108–1127 (2017).
- [11] Flick, K. E., “Back-up warning system for a vehicle and related method,” (Apr. 12 2005). US Patent 6,879,248.
- [12] Payne, G. R., “Vehicle backup monitoring and alarm system,” (Feb. 17 2004). US Patent 6,693,524.
- [13] Lediju, M. A., Trahey, G. E., Byram, B. C., and Dahl, J. J., “Short-lag spatial coherence of backscattered echoes: Imaging characteristics,” *IEEE Transactions on Ultrasonics, Ferroelectrics, and Frequency Control* **58**(7) (2011).
- [14] Graham, M. T. and Bell, M. A. L., “Photoacoustic spatial coherence theory and applications to coherence-based image contrast and resolution,” *IEEE Transactions on Ultrasonics, Ferroelectrics, and Frequency Control* **67**(10), 2069–2084 (2020).
- [15] Lediju Bell, M. A., “Photoacoustic imaging for surgical guidance: Principles, applications, and outlook,” *Journal of Applied Physics* **128**(6), 060904 (2020).
- [16] Shubert, J. and Bell, M. A. L., “Photoacoustic imaging of a human vertebra: implications for guiding spinal fusion surgeries,” *Physics in Medicine & Biology* **63**(14), 144001 (2018).
- [17] Gonzalez, E. A., Jain, A., and Bell, M. A. L., “Combined ultrasound and photoacoustic image guidance of spinal pedicle cannulation demonstrated with intact ex vivo specimens,” *Transactions on Biomedical Engineering*. Accepted.
- [18] Graham, M. T., Huang, J., Creighton, F., and Bell, M. A. L., “Simulations and human cadaver head studies to identify optimal acoustic receiver locations for minimally invasive photoacoustic-guided neurosurgery,” *Photoacoustics*, 100183 (2020).
- [19] Bell, M. A. L., Ostrowski, A. K., Li, K., Kazanzides, P., and Boctor, E. M., “Localization of transcranial targets for photoacoustic-guided endonasal surgeries,” *Photoacoustics* **3**(2), 78–87 (2015).
- [20] Kempfski, K. M., Wiacek, A., Graham, M., González, E., Goodson, B., Allman, D., Palmer, J., Hou, H., Beck, S., He, J., and Bell, M. A. L., “In vivo photoacoustic imaging of major blood vessels in the pancreas and liver during surgery,” *Journal of Biomedical Optics* **24**(12), 121905 (2019).
- [21] Gonzalez, E. A. and Bell, M. A. L., “Acoustic frequency-based differentiation of photoacoustic signals from surgical biomarkers,” in [*2020 IEEE International Ultrasonics Symposium (IUS)*], 1–4, IEEE (2020).